J. Am. Soc. Mass Spectrom. (2015) 26:1382–1387
DOI: 10.1007/s13361-015-1165-3

RESEARCH ARTICLE

Activation of Methane by the Pyridine Radical Cation and its Substituted Forms in the Gas Phase

Guohua Wu,[1,2] Hamish Stewart,[2] Zeyu Liu,[1] Yongcheng Wang,[3] Anthony J. Stace[2]

[1]Sericultural Research Institute, Jiangsu University of Science and Technology, Zhenjiang, 212018, China
[2]School of Chemistry, University of Nottingham, Nottingham, NG7 2RD, UK
[3]College of Chemistry and Chemical Engineering, Northwest Normal University, Lanzhou, 730070, China

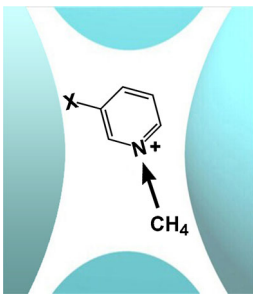

Abstract. We present an experimental study of methane activation by pyridine cation and its substituents in the gas phase. Mass spectrometric experiments in an ion trap demonstrate that pyridine cation and some of its substituent cations are able to react with methane. The deuterated methane experiment has confirmed that the hydrogen atom in the ionic product of reaction does come from methane. The collected information about kinetic isotope effects has been used to distinguish the nature of the bond activation as a hydrogen abstraction. Furthermore, experimental results demonstrated that the substituent groups on the pyridine ring can crucially influence their reactivity in methane bond activation processes. Density functional calculation (DFT) was employed to study the electronic structures of the complex and reaction mechanism of CH_4+$C_5H_5N^+$. The calculations confirmed the hypothesis from the experimental observation, namely, the reaction is rapid with no energy barrier.

Keywords: C–H activation, Density functional calculation (DFT), Gas-phase reactions, Ion trap, Methane

Received: 22 January 2015/Revised: 29 March 2015/Accepted: 10 April 2015/Published Online: 20 May 2015

Introduction

Bond activation in methane and other saturated hydrocarbons has been the subject of numerous studies to date [1–7]. Methane activation by bare transition-metal atoms and ions has also been studied extensively [8–12]; however, thermalized ground-state monoatomic 3d- and 4d-transition-metal cations generally do not react with methane because of repulsive interactions with substituent s orbitals [9, 12–15]. Methane reactions with metal cluster ions [16], metal oxide ions [17–20], metal hydrides [21], and metal complex ions [22–27] have also been extensively investigated, as has methane activation by means of ligation [28]. Schwarz et al. [29] have demonstrated that cluster size, charge state, and ligands critically affect both the reactivity and selectivity of metal-mediated bond activation processes by mass spectrometry experiments and structure calculations. This high level of activity has led to transition metals and some precious metals becoming the primary templates for methane C–H activation; however, some of the metals concerned are environmentally hazardous and the use of others may be prohibitive due to cost or lack of supply. Therefore, research on metal-free systems for methane activation is potentially valuable, even though such systems are still quite rare.

Several metal-free systems have been shown to activate molecular hydrogen, H_2. For example, Frey et al. [30] reported the similarity of certain stable carbenes and coordinatively unsaturated metal centers in the splitting of dihydrogen and ammonia. Bettinger et al. [31] extended this research to electrophilic singlet borylnitrene compounds and found that certain borylnitrenes are good reagents for the transformation of methane. Hydrogen atom abstraction from CH_4 is considered to be a key step in the oxidative dehydrogenation and dimerization of methane [32–34], and abstraction by metal-free radical cation oxides, such as $[P_4O_{10}]^+$ and $[SO_2]^+$ at room temperature have been reported by Schwarz et al. [35, 36] and de Petris et al. [37]. The gas-phase experiments on methane activation are helpful in revealing the mechanistic details of the elementary steps in the condensed phase [11].

Here, we report experimental evidence to support the pyridine cation as being uniquely efficient at activating the C–H

Electronic supplementary material The online version of this article (doi:10.1007/s13361-015-1165-3) contains supplementary material, which is available to authorized users.

Correspondence to: Guohua Wu; *e-mail:* ghwu@just.edu.cn, Anthony Stace; *e-mail:* anthony.stace@nottingham.ac.uk

bond in a study that address, for the first time, the gas-phase reactivity of the pyridine cation and its substituents with methane. The reaction between a pyridine ion and neutral methane can be described by Equation 1, which is a hydrogen-atom abstraction reaction yielding protonated pyridine $C_5H_5NH^+$ (**A**) (see Scheme 1 and Figure 1b) and a methyl radical.

$$C_5H_5N^+ + CH_4 \rightarrow C_5H_5NH^+ + CH_3 \quad (1)$$

Experimental

Methods

Experiments were performed in a quadrupole ion trap, which was interfaced with a quadrupole mass filter and two quadrupole energy deflectors. A detailed description of the apparatus has been presented elsewhere [38]. Pyridine ions and other ions of interest were generated by electron impact. The ions of interest were mass-selected by passing through a quadrupole mass filter then transmitted through an ion guide to a quadrupole ion trap, where they were allowed to react with methane. Methane was admitted directly to the ion trap via a precision leak valve at a pressure of 3×10^{-6} mbar.

Although the ions were injected into the trap with an initial kinetic energy of approximately 11 eV, once trapped, they were thermalized through multiple collisions with a helium buffer gas (99.9999%, BOC gases) prior to their reaction with methane. Following a period of isolation and reaction, precursor and product ions were scanned out of the trap in the direction of an electron multiplier, the detector of the ion trap mass spectrometer, which was located just beyond the exit end cap of the ion trap, where a mass spectrum was recorded.

Calculation Details

All molecular geometries (reactants, intermediates, transition states, and products) were fully optimized on each ground state. The electronic structures of the studied systems were investigated by using the B3LYP and Aug-cc-pVTZ basis set. The vibrational frequencies obtained at the same theoretical level were used to characterize all stationary points as either minima (the number of imaginary frequencies (NIMA)=0) or transition structure (NIMA=1). IRCs were traced from the transition state

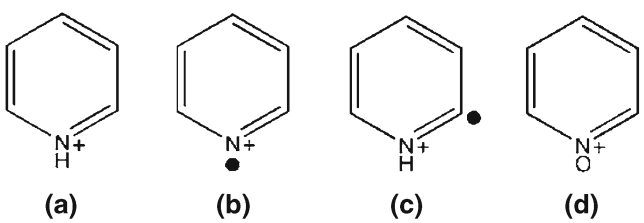

Scheme 1. Structural representations of (**A**) protonated pyridine; (**B**) ionized pyridine; (**C**) α-distonic pyridine isomer; and (**D**) the pyridine-N-oxide ion

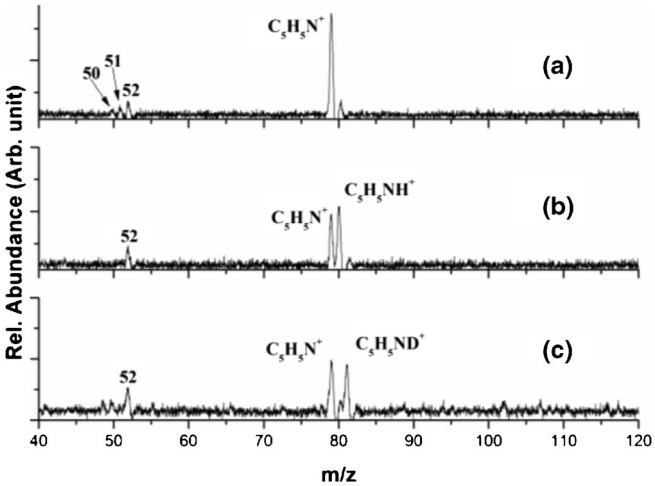

Figure 1. (**a**) Mass spectrum recorded in the ion trap for ionized pyridine and reaction products formed following the introduction of (**b**) CH_4 and (**c**) CD_4. CH_4 and CD_4 were admitted directly to the ion trap via a precision leak valve at a pressure of 3×10^{-6} mbar

(TS) toward both reactant and product directions along the imaginary mode of vibration using the algorithm developed by Gonzalez and Schlegel [39] in the mass-weighted internal coordinate system. All calculations were performed with the GAUSSIAN 03 program package [40].

Results and Discussion

It was observed that the reaction proceeds very rapidly and was almost completed during the collection period of the reactant ions (~5 ms). The almost total consumption of reactant ions suggests an unusually high level of reactivity between the pyridine ion and methane.

Since reactivity will depend quite strongly on the identities of the reactants, further studies have been undertaken to determine unambiguously the structure of the pyridine cation generated in these experiments. This step is necessary because structurally related isomers, for example from a 1,2-H shift in ionized pyridine, may be present under certain experimental conditions. Generation, isomerization, and the reactivity of pyridine radical-cations and their distonic forms have been investigated by a number of research groups [41–50]. It has been found that the conventional ionized species is more stable than its α-distonic tautomer; however, both are stable because of the presence of discrete energy minima; the large barrier towards their interconversion has been confirmed by both computational and experimental results [47]. Moreover, the tautomerism of ionized pyridine with its α-distonic ion has been found to be subject to proton-transport catalysis [50].

A distinction between ionized pyridine (**B**) from its α-distonic form (**C**) (see Scheme 1) has been identified by Schwarz and co-workers [51] on the basis of the *m/z* 28 (CH_2N^+)/26 ($C_2H_2^+$) peak branching ratio in their respective collision induced dissociation (CID) spectra. A better

differentiation between the two ions was obtained through an associative ion molecule reaction with dimethyl disulfide as a neutral reagent [50]. Moreover, the pyridine-*N*-oxide ion (**D**) (see Scheme 1) at *m/z* 95 has been observed when the α-distonic ion (**C**) was allowed to react with water in a quadrupole collision cell [48]. Under similar conditions, the pyridine radical cation (**B**) is completely unreactive. Similar behavior was seen in the present experiment (see Figure 1a) when ionized pyridine was injected into the ion trap in the absence of methane. Since the ions can be trapped for up to 1 s, they have many opportunities to collide with background water molecules. However, neither pyridine-*N*-oxide ion (**D** above) (*m/z* 95) nor $C_5H_5NH^+$ (*m/z* 80) was observed in Figure 1a, which clearly demonstrates that the ion selected and injected into the ion trap was ionized pyridine (**B**) and not expected to react with water under these experimental conditions. Confirmation that H_2O is present as a background gas has been established in other experiments we have reported [38, 52, 53], and also in this study. where it is seen to react with the 2-acetylpyridine ion (see below). To confirm that the hydrogen atom in the ionic product of Reaction 1 does come from methane rather than impurity, the fully deuterated compound, CD_4, has also been used as a neutral reagent. The only product ion $C_5H_5ND^+$ is observed (see Figure 1c), which clearly indicates the occurrence of hydrogen abstraction reaction from methane. Note that the weak signals at *m/z* 50, 51, and 52 in Figure 1 a–c are fragment ions of ionized pyridine that arise from CID.

For a better understanding of the kinetics, the time dependence of the reactant ion intensities was studied in order to evaluate rate constants for the reactivity of CH_4 and CD_4. A large excess of methane was admitted into the ion trap, thereby making it possible to determine rate constants for pseudo first order reactions. At ambient temperature and at a methane pressure of 3×10^{-6} mbar rate coefficients for the reactions of CH_4 and CD_4 with the pyridine ion are measured as 2×10^{-9} cm^3 s^{-1} and 3×10^{-10} cm^3 s^{-1} respectively, which gives an estimated kinetic isotope effect (k_H/k_D) of 5 for C–H bond activation. What has been measured here is the intermolecular kinetic isotope effect and so the value quoted is subject to experimental error. However, the fact that the ratio k_H/k_D is greater than 1 does support the view that C–H bond activation is the rate-determining step. The quoted methane pressure has been corrected to take account of the gauge's location with respect to the ion trap [38]. According to a simple two-dimensional transition state model of a three-center process [54], an isotope effect of this magnitude would imply the presence of a linear, symmetric transition state for H atom transfer. However, a more reliable conclusion would require further measurements to be made of the temperature dependence of k_H/k_D. One additional experiment performed with the trap cooled to approximately 150 K with liquid nitrogen showed the reaction between ionized pyridine and CH_4 or CD_4 as being too fast for a rate constant measurement; the reaction went almost to completion during the time allowed for collection of the reactant ion.

The enthalpy change calculated for Reaction 1 from thermodynamic data is –62.5 kJ mol^{-1} (see Table 1); this value, together with the very high rate at low temperatures, would suggest that the process is barrierless and that H-atom abstraction proceeds via the formation of a collision complex. The decrease in reaction rate with increasing temperature can then be explained in terms of a reduction in probability of the colliding molecules forming such a complex. As there appears to be no noticeable H/D scrambling in the product ion, it is proposed that any intermediate states along the reaction pathway are not long-lived.

To understand the reaction mechanisms of $C_5H_5N^+$ (B and C) and CH_4, potential energy profiles have been calculated using density functional theory (DFT). Despite the numerous strategies pursued to locate a stabilized reactant-like intermediate (IM_1) on the potential energy surface (PES) of [**B**+CH_4], no such complex was found. The transition state (TS_1) formed instantly as **B** and CH_4 collide with each other, indicating the PES is very flat in this region (see Figure 2). Hence, we can infer that the reaction is rapid with no energy barrier. The structure of TS_1 is found to be C_{2v} symmetry and its calculated energy is –5.3 kJ mol^{-1} with respect to the reactants (**B**+CH_4) (see Supplementary Table S1). The N···H distance is calculated as 2.56 Å, which is smaller than the corresponding van der Waals separation (~2.70 Å). Mulliken population analysis (MPA) shows that the charge distribution to be –0.09 e for N atom and 0.29 e for H atom in TS_1, comparing with –0.01 e for N atom and 0.23 e for H atom in the isolate reactants. Obviously, the electron transfer has occurred in TS_1 resulting from the inter-attraction of **B** and CH_4 moieties. The electrostatic interaction between N atom and H atom favors the homolytic cleavage of the C–H bond in CH_4 group to form CH_3 free radical. The transition vectors from the vibration analysis really correspond to the breaking of the C–H bond and the forming of the N–H bond (see Supplementary Figure S1). The product-like IM_2 is comprised of two moieties, **A** and CH_3, with a C_s symmetry. The relative energy is calculated to be –77.5 kJ mol^{-}

Table 1. Calculated Standard Enthalpy Changes for the Reaction of the Pyridine Ion and Its Substituted Forms with Methane (A Negative Enthalpy Means that the Reaction is Exothermic)

Reactant ion	Ion-molecule reaction	Enthalpy/kJ mol^{-1}
Pyridine	$C_5H_5N^+ + CH_4 \rightarrow C_5H_5NH^+ + CH_3$	–62.5
3-Br-pyridine	$3\text{-Br-}C_5H_4N^+ + CH_4 \rightarrow 3\text{-Br-}C_5H_4NH^+ + CH_3$	–87.5
2-Br-pyridine	$2\text{-Br-}C_5H_4N^+ + CH_4 \rightarrow 2\text{-Br-}C_5H_4NH^+ + CH_3$	–75.5
4-CH_3-pyridine	$4\text{-}CH_3\text{-}C_5H_4N^+ + CH_4 \rightarrow 4\text{-}CH_3\text{-}C_5H_4NH^+ + CH_3$	–60.5

All heats of formation of the relevant ions and radicals in the reaction schemes are taken from *J. Phys. Chem. Ref. Data* **17** (Supplement 1) (1988) [55]

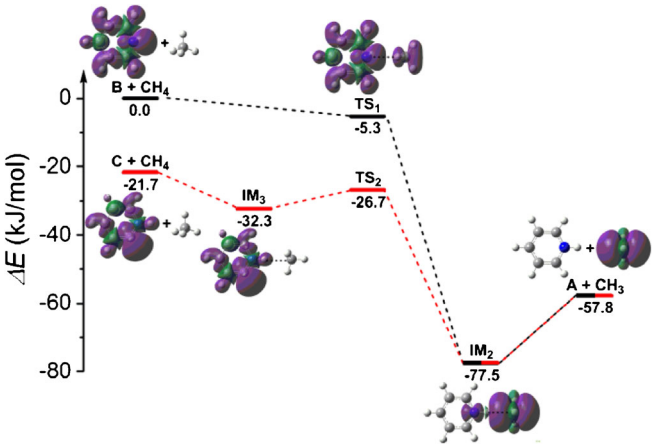

Figure 2. Calculated potential energy profiles as well as the spin distributions of the related species along the reaction pathway of $C_5H_5N^+$ (B and C) with CH_4 at the B3LYP/Aug-cc-pVTZ level of theory

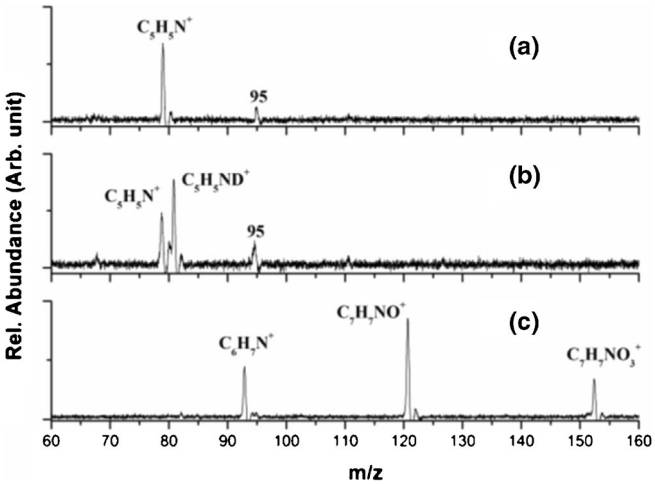

Figure 3. Ion trap mass spectra showing reactivity of the α-distonic ion of pyridine with (**a**) H_2O in the background, (**b**) CD_4 (at a pressure of 3×10^{-6} mbar), and (**c**) mass spectrum showing those products formed when the 2-acetylpyridine ion is trapped in the presence of CD_4

[1]. The C···H distance of 2.14 Å is markedly shorter than the sum of their van der Waals radii of ~2.90 Å, showing a strongly electrostatic interaction between **A** and CH_3 free radical. The C–H length and H–C–H angle in CH_3 moiety of product-like IM_2 are 1.08 Å and ~119°, respectively, which are extremely similar to that of the isolate CH_3 free radical. This complex can split to produce the products (**A** and CH_3) with the dissociation energy of 19.7 kJ mol^{-1}. The value of calculated heat of the reaction is exothermic by –57.8 kJ mol^{-1}, which is in agreement with the standard enthalpy changes calculated with the literature value (–62.5 kJ mol^{-1}) [55].

To investigate the reactivity of the distonic isomer (**C** in Scheme 1) with methane, pyridine was replaced by 2-acetylpyridine, for which dissociative ionization is known to give the distonic ion [50]. A mass spectrum in the absence of methane is shown in Figure 3a. In addition to the distonic ion, the pyridine-*N*-oxide ion (**D** in Scheme 1) has also been produced by a reaction of $C_5H_5N^+$ with background water molecules [49]. However, a large difference of the *m/z* 95 product ions from reaction with water between our experiment and the former literature might be caused by the different experimental conditions, for example, the kinetic energy of the α-distonic pyridine isomer, reaction time, and water pressures in our ion trap and the reaction cell in reference [47]. As seen in Figure 3b, $C_5H_5ND^+$ is the main product following the reaction of the α-distonic ion with CD_4. However, it should be noted that the reaction with methane is far slower than that of methane with ionized pyridine under the same experimental conditions.

The theoretical analysis shows that the reaction pathway of C with CH_4 is different from that of B with CH_4 (see Figure 2). A stabilized reactant-like intermediate (IM_3) is formed when C and CH_4 approach each other. This initially formed ion/molecule complex has *C*s symmetry, and its energy is –10.6 kJ mol^{-1} relative to the reactants (C+CH_4) (see Supplementary Table S2). The C···H distance of 2.27 Å is shorter than the sum of their van der Waals radii (~2.90 Å) but longer than the normal C–H bond length, indicating the interaction between C and CH4 is electrostatic in nature. The inference can also be drawn from the N–H length in C moiety and C–H length in CH_4 moiety of 1.02 and 1.09 Å, respectively, which are similar to those parameters in the isolate reactants. The structure of transition state in this pathway (TS_2) is found to be also C_s geometry. The activation barrier of TS_2 is 5.5 kJ mol⁻with respect to the intermediate, IM_3. The C–H distances between two moieties are 1.51 and 1.22 Å, respectively (see Supplementary Figure S2). Clearly, TS_2 is a tightly bonded structure. Similar to what was seen in the reaction of B with CH_4, the electrostatic interaction between C atom and H atom in TS_2 favors the homolytic cleavage of the C–H bond in CH_4 group. The transition vectors from the vibration analysis demonstrate this point well (Supplementary Figure S2). The homolytic cleavage of the C–H bond results in the product-like IM_2, and the reaction enters the same channel as the reaction of B with CH_4 after that.

It was well known that for the reaction of a radical cation with CH_4, the spin distribution is very important. The spin distributions of the related species along the reaction pathways of $C_5H_5N^+$ (B and C) with CH_4 are displayed in Figure 2. As expected, the distributions of spin density obtained by B3LYP/Aug-cc-pVTZ indicate that radical (unpaired) electron almost spreads over the region of the $C_5H_5N^+$ (B and C) moiety in reactant-like intermediate (IM_3) and the region of CH_3 group in product-like intermediate (IM_2), whereas the spin densities distribute around the whole complex for the transition states (TS_1 and TS_2).

Different from the reaction of B with CH_4, the stabilized reactant-like intermediate (IM_3) is explicitly located at the PES of [C+CH_4]. It can be deduced that the reaction of C with CH_4 is slower than that of B with CH_4, considering that the rate-limiting step in the reaction pathway of the former needs to get over 5.5 kJ mol^{-1} energy barrier.

In order to study the influence substitution has on reactivity with methane, a series of pyridine radical ions were generated with substituents at the meta-, para-, or ortho-position. With injection of

the 3-bromopyridine ion into the ion trap, hydrogen-atom abstraction was observed concomitant with the formation of a methyl radical (Figure 4a), and this reaction was also found to be much faster at low temperature (~150 K). Since Br is a weak electron-withdrawing group, the presence of the atom on pyridine may actually stabilize the cation by delocalizing electron density which, in turn, may reduce reactivity. This was indeed found to be the case for the 2-bromopyridine cation, where the H-atom abstraction yield was very low. However, as Table 1 shows, the reactions of both ions are predicted to be very exothermic. Similar finding were found for 2-acetylpyridine (Figure 3c), which was observed to be completely unreactive towards methane under our experimental conditions. Instead, only an O_2 adduct ion ($C_7H_7NO_3^+$ at *m/z* 153) and a fragment ion at *m/z* 93 ($C_6H_7N^+$) from the collision-induced loss of CO from the precursor ion were observed. The reactivity of 2-acetylpyridine may also be influenced by steric hindrance. Finally, the reactivity of 4-methylpyridine was studied. In comparison to the bare pyridine cation, the product yield from this ion was low, even though the reaction was again predicted to be exothermic (see Table 1). The effect of substitution probably has a similar effect to that observed for the 2-substituted isomers since methyl is a weak electron donating group.

Since pyridine is an aromatic heterocyclic compound and most strongly resembles benzene in its structure and stability, it was considered appropriate to compare the reactivity of methane with other ionized single-ring homocyclic and heterocyclic molecules. Cations from furan (C_4H_4O), pyrrole (C_4H_5N), thiophene (C_4H_4S), pyrrolidine (C_4H_9N), piperidine ($C_5H_{11}N$), benzene (C_6H_6), toluene (C_7H_8), and benzonitrile (C_7H_5N) were generated by electron impact ionization, mass-selected, and injected into the ion trap where they were allowed to react with methane. These ions were mostly unreactive towards methane and in those instances where fragments were seen, collisional excitation was most probably responsible. The only exception was ionized benzene, which reacted with methane to give $C_7H_7^+$ (reaction (2)) by associative dissociation.

$$C_6H_6^+ + CH_4 \rightarrow C_7H_7^+ + H_2 + H \quad (2)$$

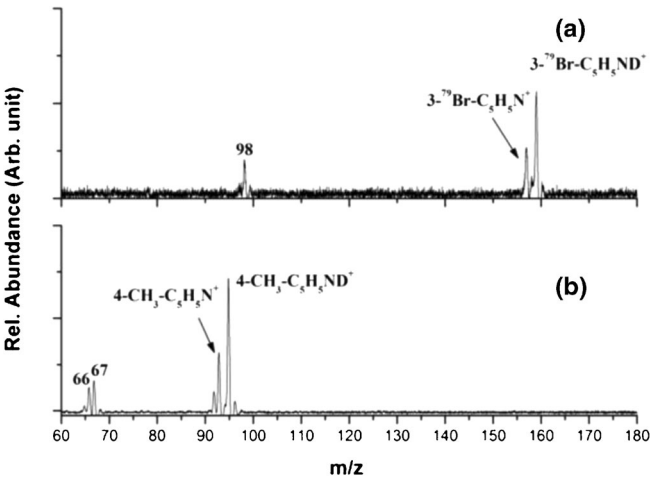

Figure 4. Ion trap mass spectra showing the products formed following reactions between CD_4 (at a pressure of 3×10^{-6} mbar) and (**a**) the 3-bromo-pyridine cation; (**b**) the 4-methyl-pyridine cation

Conclusion

A new nonmetallic molecular system has been identified that will activate methane in the gas phase under mild conditions. Results have been presented showing for the first time that a reaction between ionised pyridine and methane can produce the methyl radical. In addition, it has been seen that substituted forms of the pyridine ion can undergo a similar reaction, but that the degree of reactivity is influenced by the nature and position of the substituent. If these or similar processes could be sustained in the condensed phase, they may offer a route to the production of larger hydrocarbons from methane. At the very least, it has been shown that mass spectrometry can yield valuable insight into the mechanism of methane C–H bond activation.

Acknowledgments

The authors thank EPSRC and the University of Nottingham for financial support. They are also very grateful to the Jiangsu Specially Appointed Professor Program (Sujiaoshi[2012]27).

References

1. Cui, W.H., Wayland, B.B.: Activation of C–H/H–H Bonds by rhodium(II) porphyrin bimetalloradicals. J. Am. Chem. Soc. **126**, 8266–8274 (2004)
2. Hoyt, H.M., Michael, F.E., Bergman, R.G.: c–h bond activation of hydrocarbons by an imidozirconocene complex. J. Am. Chem. Soc. **126**, 1018–1019 (2004)
3. Adams, C.S., Legzdins, P., Tran, E.: Thermal activation of hydrocarbon c–h bonds by tungsten alkylidene complexes. J. Am. Chem. Soc. **123**, 612–624 (2001)
4. Fokin, A.A., Schreiner, P.R., Gunchenko, P.A., Peleshanko, S.A., Shubina, T.E., Isaev, S.D., Tarasenko, P.V., Kulik, N.I., Schiebel, H.M., Yurchenko, A.G.: Oxidative single-electron transfer activation of sigma-bonds in aliphatic halogenation reactions. J. Am. Chem. Soc. **122**, 7317–7326 (2000)
5. Arndtsen, B.A., Bergman, R.G.: Unusually mild and selective hydrocarbon c–h bond activation with positively charged iridium(iii) complexes. Science **270**, 1970–1973 (1995)
6. Schultz, R.H., Bengali, A.A., Tauber, M.J., Weiller, B.H., Wasserman, E.P., Kyle, K.R., Moore, C.B., Bergman, R.G.: IR flash kinetic spectroscopy of C–H bond activation of cyclohexane-d_0 and -d_{12} by Cp*Rh(CO)$_2$ in liquid rare gases: kinetics, thermodynamics, and an unusual isotope effect. J. Am. Chem. Soc. **116**, 7369–7377 (1994)
7. Schwarz, H.: Chemistry with methane: concepts rather than recipes. Angew. Chem. Int. Ed. **50**, 10096–10115 (2011)
8. Schröder, D., Schwarz, H.: FeO^+ activates methane. Angew. Chem. Int. Ed. Engl. **29**, 1433–1434 (1990)
9. Weisshaar, J.C.: Bare transition metal atoms in the gas phase: reactions of M, M^+, and M^{2+} with hydrocarbons. Acc. Chem. Res. **26**, 213–219 (1993)
10. Marcalo, J., Santos, M., Matos, A.P., Gibson, J.K., Haire, R.G.: Gas-phase reactions of doubly charged lanthanide cations with alkanes and alkenes. Trends in metal(2+) reactivity. J. Phys. Chem. A **112**, 12647–12656 (2008)
11. Schwarz, H., Schröder, D.: Concepts of metal-mediated methane functionalization. an intersection of experiment and theory. Pure Appl. Chem. **72**, 2319–2332 (2000)

12. Irion, M.P., Selinger, A.: FTMS Studies of Sputtered Metal Cluster Ions: (II) The Chemistry of Ni_n^+ with C_2H_4 and CH_4 at Long Timescales. Ber. Bunsenges. Phys. Chem. **93**, 1408–1412 (1989)
13. Armentrout, P.B., Beauchamp, J.L.: The chemistry of atomic transition-metal ions: insight into fundamental aspects of organometallic chemistry. Acc. Chem. Res. **22**, 315–321 (1989)
14. Buckner, S.W., McMahon, T.J., Byrd, G.D., Freiser, B.S.: Gas-phase reactions of Nb^+ and Ta^+ with alkanes and alkenes. C–H bond activation and ligand-coupling mechanisms. Inorg. Chem. **28**, 3511–3518 (1989)
15. Perry, J.K., Ohanessian, G., Goddard III, W.A.: Mechanism and energetics for dehydrogenation of methane by gaseous iridium ions. Organometallics **13**, 1870–1877 (1994)
16. Koszinowski, K., Schlangen, M., Schröder, D., Schwarz, H.: C–H- and N–H-activation by gaseous Rh_2^+ and $PtRh^+$ cluster ions. Int. J. Mass Spectrom. **237**, 19–23 (2004)
17. Schröder, D., Schwarz, H.: c–h and c–c bond activation by bare transition-metal oxide cations in the gas-phase. Angew. Chem. Int. Ed. Engl. **34**, 1973–1995 (1995)
18. Feyel, S., Döbler, J., Schröder, D., Sauer, J., Schwarz, H.: Thermal activation of methane by tetranuclear $[V_4O_{10}]^+$. Angew. Chem. Int. Ed. Engl. **45**, 4681–4685 (2006)
19. Wang, Z.-C., Dietl, N., Kretschmer, R., Ma, J.-B., Weiske, T., Schlangen, M., Schwarz, H.: Direct conversion of methane into formaldehyde mediated by $[Al2O3].^+$ at room temperature. Angew. Chem. Int. Ed. **51**, 3703–3707 (2012)
20. Wang, Z.-C., Weiske, T., Kretschmer, R., Schlangen, M., Kaupp, M., Schwarz, H.: Structure of the oxygen-rich cluster cation $Al2O7^+$ and its reactivity toward methane and water. J. Am. Chem. Soc. **133**, 16930–16937 (2011)
21. Schlangen, M., Schwarz, H.: Thermal activation of methane by group 10 metal hydrides MH^+: The same and not the same. Angew. Chem. Int. Ed. Engl. **46**, 5614–5617 (2007)
22. Metz, R.B.: Photofragment spectroscopy of covalently bound transition metal complexes: a window into C–H and C–C bond activation by transition metal ions. Int. Rev. Phys. Chem. **23**, 79–108 (2004)
23. Schröder, D., Schwarz, H.: Gas-phase activation of methane by ligated transition-metal cations. Proc. Natl. Acad. Sci. U. S. A. **105**, 18114–18119 (2008)
24. Schlangen, M., Schröder, D., Schwarz, H.: Pronounced ligand effects and the role of formal oxidation states in the nickel-mediated thermal activation of methane. Angew. Chem. Int. Ed. Engl. **46**, 1641–1644 (2007)
25. Butschke, B., Schlangen, M., Schwarz, H., Schröder, D.: C–H bond activation of methane with gaseous $[(CH_3)Pt(L)]^+$ complexes (L = pyridine, bipyridine, and phenanthroline). Z. Naturforsch. B **62**, 309–313 (2007)
26. Yoshizawa, K., Suzuki, A., Yamabe, T.: Inversion of methane on transition-metal complexes: a possible mechanism for inversion of stereochemistry. J. Am. Chem. Soc. **121**, 5266–5273 (1999)
27. Fu, R., Reilly, M.E.O., Nielsen, R.J., Goddard III, W.A., Gunnoe, T.B.: Rhodium Bis(quinolinyl)benzene complexes for methane activation and functionalization. Chem. Eur. J. **21**, 1286–1293 (2015)
28. Carpenter, C.J., van Koppen, P.A.M., Bowers, M.T., Perry, J.K.: The role of the cyclopentadienyl ligand in the sigma-bond activation of methane. J. Am. Chem. Soc. **122**, 392–393 (2000)
29. Schwarz, H.: How and why do cluster size, charge state, and ligands affect the course of metal-mediated gas-phase activation of methane? Isr. J. Chem. **54**, 1413–1431 (2014)
30. Frey, G.D., Lavallo, V., Donnadieu, B., Schoeller, W.W., Bertrand, G.: Facile splitting of hydrogen and ammonia by nucleophilic activation at a single carbon center. Science **316**, 439–441 (2007)
31. Bettinger, H.F., Filthaus, M., Bornemann, H., Oppel, I.M.: Metal-free conversion of methane and cycloalkanes to amines and amides by employing a borylnitrene. Angew. Chem. Int. Ed. **47**, 4744–4747 (2008)
32. Lunsford, J.H.: The catalytic oxidative coupling of methane. Angew. Chem. Int. Ed. Engl. **34**, 970–980 (1995)
33. Fokin, A.A., Schreiner, P.R.: Metal-free, selective alkane functionalizations. Adv. Synth. Catal. **345**, 1035–1052 (2003)
34. Lersch, M., Tilset, M.: Mechanistic aspects of C–H activation by Pt complexes. Chem. Rev. **105**, 2471–2526 (2005)
35. Dietl, N., Engeser, M., Schwarz, H.: Room-temperature C–H bond activation of methane by bare $[P_4O_{10}]^+$. Angew. Chem. Int. Ed. Engl. **48**, 4861–4863 (2009)
36. Dietl, N., Troiani, A., Schlangen, M., Ursini, O., Angelini, G., Apeloig, Y., de Petris, G., Schwarz, H.: Mechanistic aspects of gas-phase hydrogen-atom transfer from methane to $[CO]C^+$ and $[SiO]C^+$: why do they differ? Chem. Eur. J. **19**, 6662–6669 (2013)
37. de Petris, G., Troiani, A., Rosi, M., Angelini, G., Ursini, O.: Methane activation by metal-free radical cations: experimental insight into the reaction intermediate. Chem. Eur. J. **15**, 4248–4252 (2009)
38. Wu, G., Chapman, D., Stace, A.J.: Trapping and recording the collision- and photo-induced fragmentation patterns of multiply charged metal complexes in the gas phase. Int. J. Mass Spectrom. **262**, 211–219 (2007)
39. Gonzalez, C., Schlegel, H.B.: Reaction path following in mass-weighted internal coordinates. J. Phys. Chem. **94**, 5523–5527 (1990)
40. Frisch, M.J., Trucks, G.W., Schlegel, H.B., Scuseria, G.E., Robb, M.A., Cheeseman, J.R., Montgomery, J.A., Jr., Vreven, T., Kudin, K.N., Burant, J.C., Millam, J.M., Iyengar, S.S., Tomasi, J., Barone, V., Mennucci, B., Cossi, M., Scalmani, G., Rega, N., Petersson, G.A., Nakatsuji, H., Hada, M., Ehara, M., Toyota, K., Fukuda, R., Hasegawa, J., Ishida, M., Nakajima, T., Honda, Y., Kitao, O., Nakai, H., Klene, M., Li, X., Knox, J.E., Hratchian,H.P., Cross, J.B., Adamo, C., Jaramillo, J., Gomperts, R., Stratmann, R.E., Yazyev, O., Austin, A.J., Cammi, R., Pomelli, C., Ochterski, J.W., Ayala, P.Y., Morokuma, K., Voth, G.A., Salvador, P., Dannenberg, J.J., Zakrzewski, V.G., Dapprich, S., Daniels, A.D., Strain, M.C., Farkas, O., Malick, D.K., Rabuck, A.D., Raghavachari, K., Foresman, J.B., Ortiz, J.V., Cui, Q., Baboul, A.G., Clifford, S., Cioslowski, J., Stefanov, B.B., Liu, G., Liashenko, A., Piskorz, P., Komaromi, I., Martin, R.L., Fox, D.J., Keith, T., Al-Laham, M.A., Peng, C.Y., Nanayakkara, A., Challacombe, M., Gill, P.M.W., Johnson, B., Chen, W., Wong, W., Gonzalez, C., Pople, J.A.: Gaussian 03, revision E.01; Gaussian, Inc.: Pittsburgh, PA: Gaussian, Inc.: Wallingford CT, Gaussian 03, (Revision E.01) (2004)
41. Alvarez, E., Conejero, S., Lara, P., Lopez, J.A., Paneque, M., Petronilho, A., Poveda, M.L., del Rio, D., Serrano, O., Carmona, E.: Rearrangement of Pyridine to Its 2-Carbene Tautomer Mediated by Iridium. J. Am. Chem. Soc. **129**, 14130–14131 (2007)
42. Alvarez, E., Conejero, S., Paneque, M., Petronilho, A., Poveda, M.L., Serrano, O., Carmona, E.: Iridium(III)-induced isomerization of 2-substituted pyridines to *N*-heterocyclic carbenes. J. Am. Chem. Soc. **128**, 13060–13061 (2006)
43. Buil, M.L., Esteruelas, M.A., Garces, K., Olivan, M., Onate, E.: Understanding the formation of n–h tautomers from alpha-substituted pyridines: tautomerization of 2-ethylpyridine promoted by osmium. J. Am. Chem. Soc. **129**, 10998–10999 (2007)
44. Kunz, D.: Synthetic routes to *n*-heterocyclic carbene complexes: pyridine-carbene tautomerizations. Angew. Chem. Int. Ed. **46**, 3405–3408 (2007)
45. Lavorato, D., Terlouw, J.K., McGibbon, G.A., Dargel, T.K., Koch, W., Schwarz, H.: Generation of neutral and cationic hydrogen shift isomers of pyridine: a combined experimental and computational investigation. Int. J. Mass Spectrom. **179/180**, 7–14 (1998)
46. Karapanayiotis, T., Dimopoulos-Italiano, G., Bowen, R.D., Terlouw, J.K.: Reactions of ionized pyridazine, aminopyrazine, and aminopyridine and their isomeric alpha-distonic ions. Int. J. Mass Spectrom. **236**, 1–9 (2004)
47. Gerbaux, P., Trikoupis, M.A., Lavorato, D.J., Flammang, R., Terlouw, J.K.: Hydrogen-shift isomers of ionic and neutral hydroxypyridines: a combined experimental and computational investigation. Int. J. Mass Spectrom. **217**, 1–22 (2002)
48. Gerbaux, P., Barbieux-Flammang, M., Terlouw, J.K., Flammang, R.: Definitive characterization of some $C_5H_5N^{\cdot+}$ and $C_6H_7N^{\cdot+}$ radical cations by associative ion-molecule reactions. Int. J. Mass Spectrom. **206**, 91–103 (2001)
49. Trikoupis, M.A., Lavorato, D.J., Terlouw, J.K., Ruttink, P.J.A., Burgers, P.C.: Lowering large 1,2-H shift barriers by proton-transport catalysis: the challenging case of the pyridine radical cation. Eur. Mass Spectrom. **5**, 431–439 (1999)
50. Gerbaux, P., Barbieux-Flammang, M., Van Haverbeke, Y., Flammang, R.: Characterization of ionized heterocyclic carbenes by ion-molecule reactions. Rapid Commun. Mass Spectrom. **13**, 1707–1711 (1999)
51. Lavorato, D., Terlouw, J.K., Dargel, T.K., Koch, W., McGibbon, G.A., Schwarz, H.: Observation of the Hammick intermediate: reduction of the pyridine-2-ylid ion in the gas phase. J. Am. Chem. Soc. **118**, 11898–11904 (1996)
52. Wu, G., Norris, C., Stewart, H., Cox, H., Stace, A.J.: State-resolved UV photofragmentation spectrum of the metal dication complex $[Zn(pyridine)_4]^{2+}$. Chem. Commun. **35**, 4153–4155 (2008)
53. Cox, H., Norris, C., Wu, G., Guan, J., Hessey, S., Stace, A.J.: Evidence of zinc superoxide formation in the gas phase: comparisons in behavior between ligated Zn(I/II) and Cu(I/II) with regard to the attachment of O_2 or H_2O. Dalton Trans. **40**, 11200–11210 (2011)
54. Westheimer, F.H.: The magnitude of the primary kinetic isotope effect for compounds of hydrogen and deuterium. Chem. Rev. **61**, 265–273 (1961)
55. Lias, S.G., Bartmess, J.E., Liebman, J.F., Holmes, J.L., Levin, R.D., Mallard, W.G.: J. Phys. Chem. Ref. Data **17**(Suppl. 1), 1–861 (1988)